

Decay mechanisms of single particle excitations in bulk metals and at metal surfaces

E. V. Chulkov

Departamento de Física de Materiales UPV/EHU and Centro Mixto CSIC-UPV/EHU,
Donostia International Physics Center (DIPC), San Sebastián/Donostia, Spain

fundación

DONOSTIA INTERNATIONAL
PHYSICS CENTER



eman ta zabal zazu



euskal herriko
unibertsitatea

universidad
del pais vasco



**Strong
Correlations
and ARPES:
Recent
Progress in
Theory and
Experiment**

Dresden, Germany
April 4-8, 2005



Outline

1. Motivation
2. Sketch of theory
3. Decay mechanisms
4. Results
5. Conclusions

Motivation

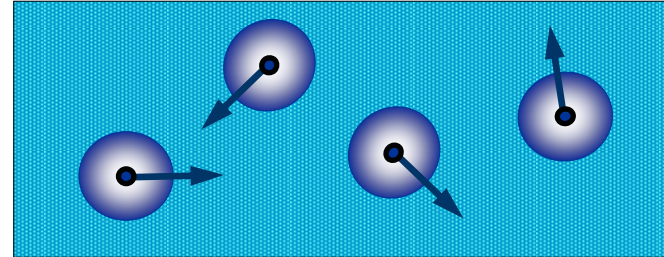
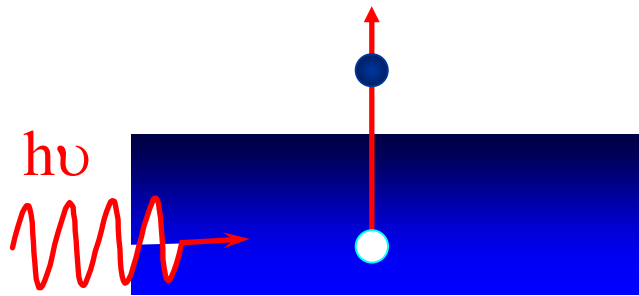
The accurate description of electronic structure is of paramount importance for understanding many properties of different materials. This description usually consist of *two* steps.

First, electronic structure is calculated in terms of “non-interacting” electrons. Common practice is the use of DFT (LDA, GGA,...) or some model hamiltonians.

Second, by using the DFT one-electron energies and wave functions the electron self-energy (Σ) is evaluated to correct the DFT electronic structure.

Majority of the Σ calculations have been done for $\text{Re}\Sigma$ while $\text{Im}\Sigma$ has been addressed significantly less.

Lifetime of quasiparticles



Interactions between quasiparticles limit how long the corresponding quantum states retain their identity: a quasiparticle is said to have a **lifetime** which sets the duration of the excitation. In combination with the velocity, this lifetime determines the **mean free path**, a measure of influence of the excitation

Importance of lifetime

- charge and spin transport in bulk materials, across interfaces, and at surfaces
- electron dynamics and energy transfer
- localization
- surface photochemistry and catalitical reactions

In general case the decay rate (lifetime broadening) of a quasiparticle measured experimentally can be written as

$$\Gamma = \Gamma_{e-e} + \Gamma_{e-ph} + \Gamma_{e-def} + \Gamma_{corr}$$

Γ_{e-e} - the inverse lifetime contribution due to inelastic electron-electron scattering

Γ_{e-ph} - the contribution from electron-phonon interaction

Γ_{e-def} - the contribution from electron-defect scattering events

Γ_{e-corr} - energy and momentum corrections due to the finite experimental resolution

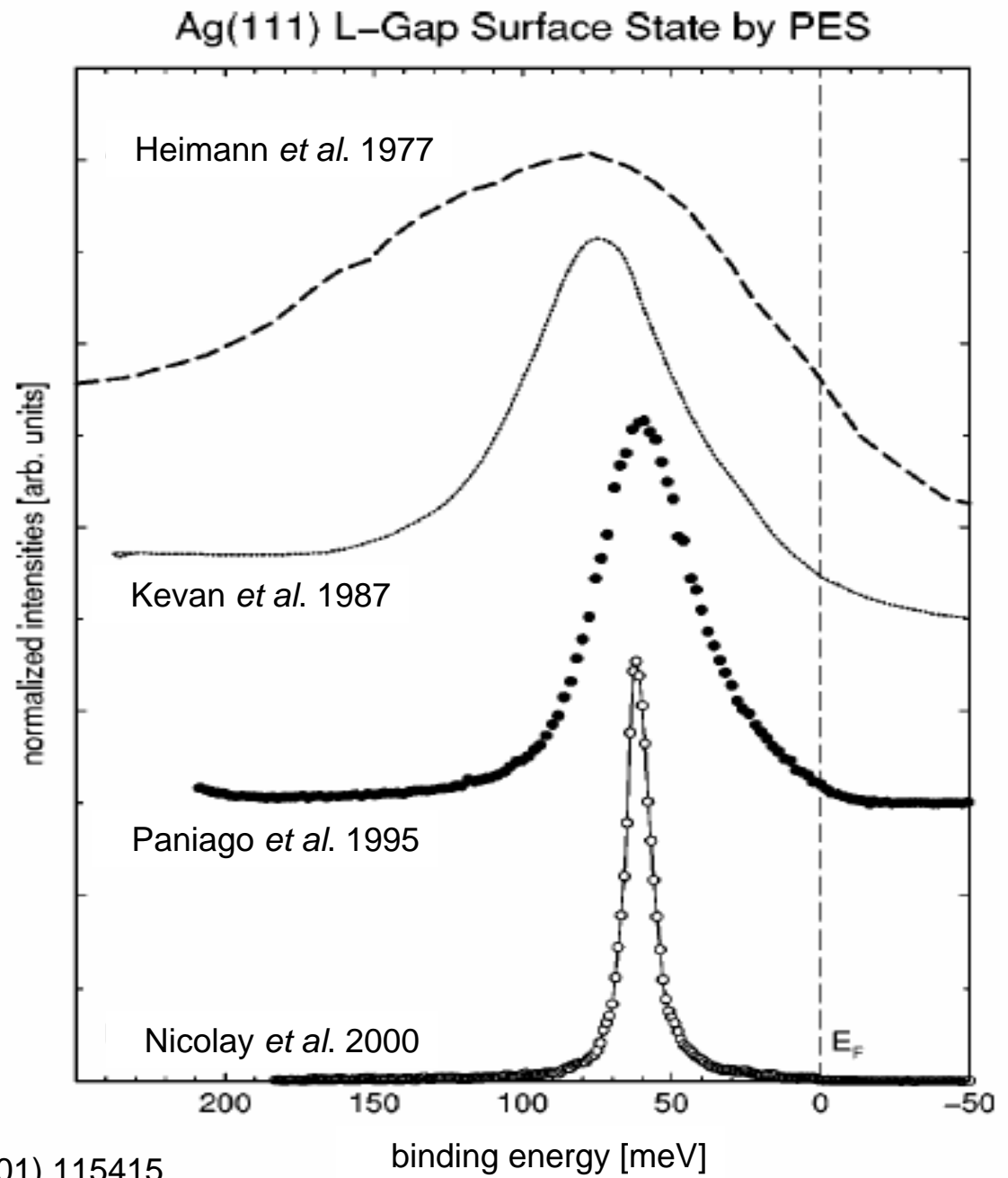
In all spectroscopies, there are two levels of interpretation. The lower level focuses on positions of spectral features. The higher, and more problematic, level focuses on intensities and shapes...

My mood of skepticism applies largely to quantitative interpretations of linewidths in terms of quasiparticle lifetimes...

The moral here is that, even on a material as well understood and easy to prepare as Cu, a very high degree of sample perfection is required if we are to avoid extraneous broadening mechanisms.

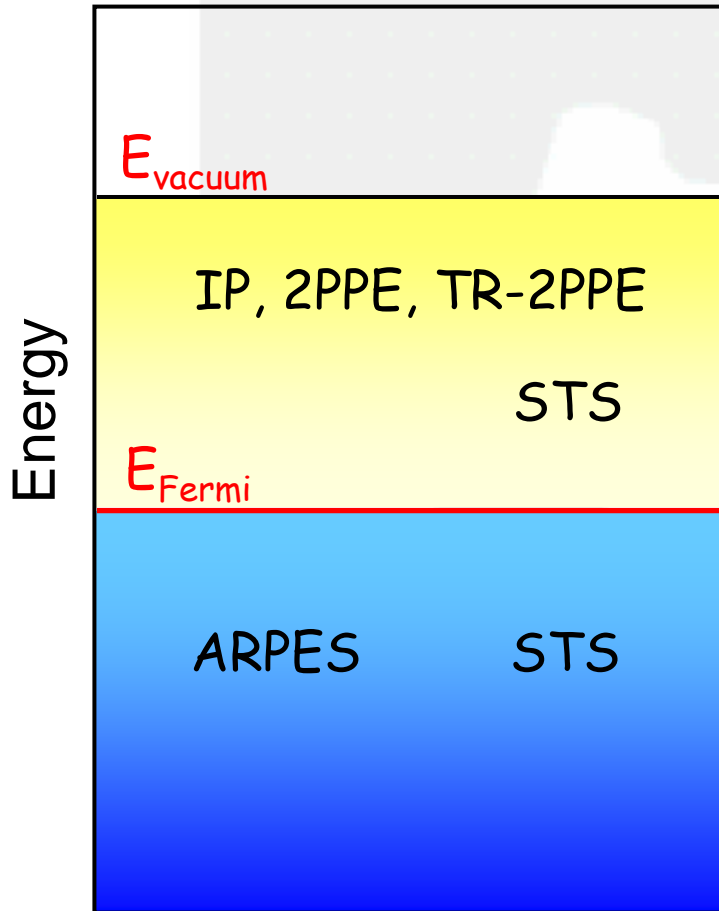
N.V.Smith. Comments Cond. Mat. Phys. 1992. Vol 15, Nos. 5&6, pp. 263-272

Experimental linewidths change quickly with time!



from F.Reinert *et al.*, PRB **63** (2001) 115415.

Experimental Methods



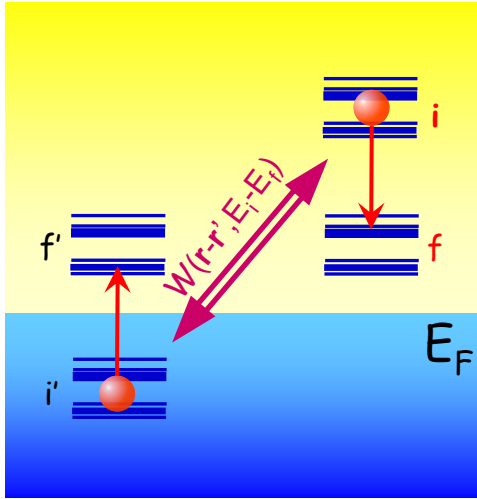
- Time-Resolved Two-Photon Photoemission (TR-2PPE)
- Two-Photon Photoemission (2PPE)
- Inverse Photoemission (IP)

• Scanning Tunneling Spectroscopy (STS)

• Angle-Resolved Photoemission Spectroscopy (PES)

2. Sketch of theory: e-e interaction

- Lifetime $\tau^{-1} = -2 \int d\mathbf{r} d\mathbf{r}' \phi_i^*(\mathbf{r}) \text{Im}\Sigma(\mathbf{r},\mathbf{r}';\varepsilon_i) \phi_i(\mathbf{r}')$



- Lifetime – Screened interaction

$$\tau^{-1} = -2 \sum_f' \int d\mathbf{r} \int d\mathbf{r}' \phi_i^*(\mathbf{r}) \phi_f^*(\mathbf{r}') \text{Im}W(\mathbf{r},\mathbf{r}';\omega) \phi_i(\mathbf{r}') \phi_f(\mathbf{r})$$

- Self-energy

$$\text{Im}\Sigma(\mathbf{r},\mathbf{r}';\varepsilon_i > E_F) = \sum_{E_F \leq \varepsilon_f \leq \varepsilon_i}' \phi_f^*(\mathbf{r}') \text{Im}W(\mathbf{r},\mathbf{r}';\varepsilon_i - \varepsilon_f) \phi_f(\mathbf{r})$$

- Screened Interaction

$$W(\mathbf{r},\mathbf{r}';\omega) = V(\mathbf{r}-\mathbf{r}') + \int d\mathbf{r}_1 \int d\mathbf{r}_2 [V(\mathbf{r}_1-\mathbf{r}_2) + \mathbf{K}^{\text{xc}}(\mathbf{r}_1,\mathbf{r}_2,\omega)] \chi(\mathbf{r}_1,\mathbf{r}_2,\omega) V(\mathbf{r}_2-\mathbf{r}')$$

- Response function

$$\chi(\mathbf{r},\mathbf{r}';\omega) = \chi^0(\mathbf{r},\mathbf{r}';\omega) + \int d\mathbf{r}_1 \int d\mathbf{r}_2 \chi^0(\mathbf{r},\mathbf{r}_2,\omega) [V(\mathbf{r}_1-\mathbf{r}_2) + \mathbf{K}^{\text{xc}}(\mathbf{r}_1,\mathbf{r}_2,\omega)] \chi(\mathbf{r}_2,\mathbf{r}';\omega)$$

where

$$\chi^0(\mathbf{r},\mathbf{r}';\omega) = 2 \sum_{i,j} \frac{\theta(E_F - \varepsilon_i) - \theta(E_F - \varepsilon_j)}{\varepsilon_i - \varepsilon_j + (\omega + i\eta)} \phi_i(\mathbf{r}) \phi_j^*(\mathbf{r}) \phi_j(\mathbf{r}') \phi_i^*(\mathbf{r}')$$

2. Sketch of theory: Electron-phonon (e-ph) interaction

Electron-phonon coupling matrix element

$$g_{q,\nu}^{i,f} \equiv \sqrt{\frac{1}{2 \cdot M \cdot \omega_q^\nu}} \cdot \left\langle \phi_i^0 \left| \sum_{\mu} \vec{\epsilon}_q^{\nu,\mu} \cdot \vec{\nabla}_{R_\mu} V_{e-ion}^q \right| \phi_f^0 \right\rangle$$

Eliashberg function

$$\alpha^2 F_{\vec{k}_i}(\omega) \equiv \sum_{\vec{q},\nu} |g_{q,\nu}^{i,f}|^2 \cdot \delta(\epsilon_{\vec{k}_i}^{el} - \epsilon_{\vec{k}_f}^{el}) \cdot \delta(\omega - \omega_q^\nu)$$

Quasi-elastic approximation

$$\delta(\epsilon_{\vec{k}_i}^{el} - \epsilon_{\vec{k}_f}^{el} \pm \omega_q^\nu) \approx \delta(\epsilon_{\vec{k}_i}^{el} - \epsilon_{\vec{k}_f}^{el})$$

E-ph contribution to the electronic linewidth

$$\Gamma_{\vec{k}_i} = 2\pi \cdot \int_0^\infty \alpha^2 F_{\vec{k}_i}(\omega) \cdot [2 \cdot n_B(\omega) + 1 + f(\epsilon_{\vec{k}_i} + \omega) - f(\epsilon_{\vec{k}_i} - \omega)] \cdot d\omega$$

E-ph contribution at high temperatures ($T \rightarrow \infty$)

$$\Gamma_{\vec{k}_i} \cong 2\pi \cdot K_B \cdot T \cdot \lambda$$

E-ph contribution at $T=0$ K

$$\Gamma_{\vec{k}_i} \cong 2\pi \cdot \int_0^{\epsilon_{\vec{k}_i}} \alpha^2 F_{\vec{k}_i}(\omega) d\omega$$

E-ph coupling constant

$$\lambda = 2 \cdot \int_0^\infty \frac{\alpha^2 F_{\vec{k}_i}(\omega)}{\omega} \cdot d\omega$$

Calculations of a lifetime for
excited electrons (holes) in

Bulk states

Surface states

Image states

Quantum well states

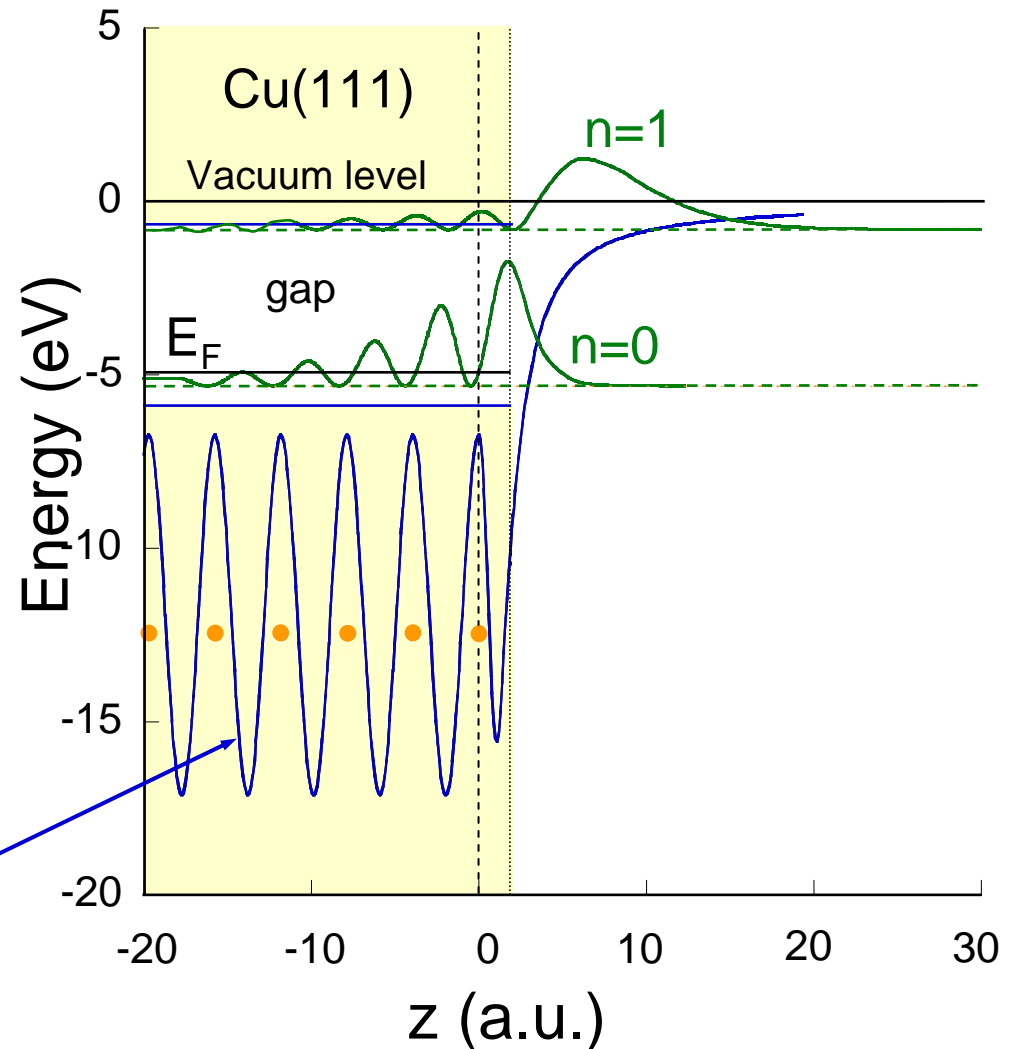
and at Adsorbates

Contributions to the
quasiparticle decay rate:

Electron-electron

Electron-phonons

Surf. Sci. **391**, L1217 (1997);
437, 330 (1999)



Model potential

3. Decay mechanisms

(electron-electron contribution)

$$\tau^{-1} = -2 \sum_f' \int d\mathbf{r} \int d\mathbf{r}' \phi_i^*(\mathbf{r}) \phi_f^*(\mathbf{r}') \text{Im}W(\mathbf{r}, \mathbf{r}'; \omega) \phi_i(\mathbf{r}') \phi_f(\mathbf{r})$$

- 1) Initial State $\phi_i(\mathbf{r})$ } Overlap of the initial and final states wave functions.
Final State $\phi_f(\mathbf{r})$ } Important difference between **intra**-band and **inter**-band transitions arises.

2) Final States Effect

a) "Phase space": number of final states in momentum space

b) Density of final states: distribution of final states in momentum space

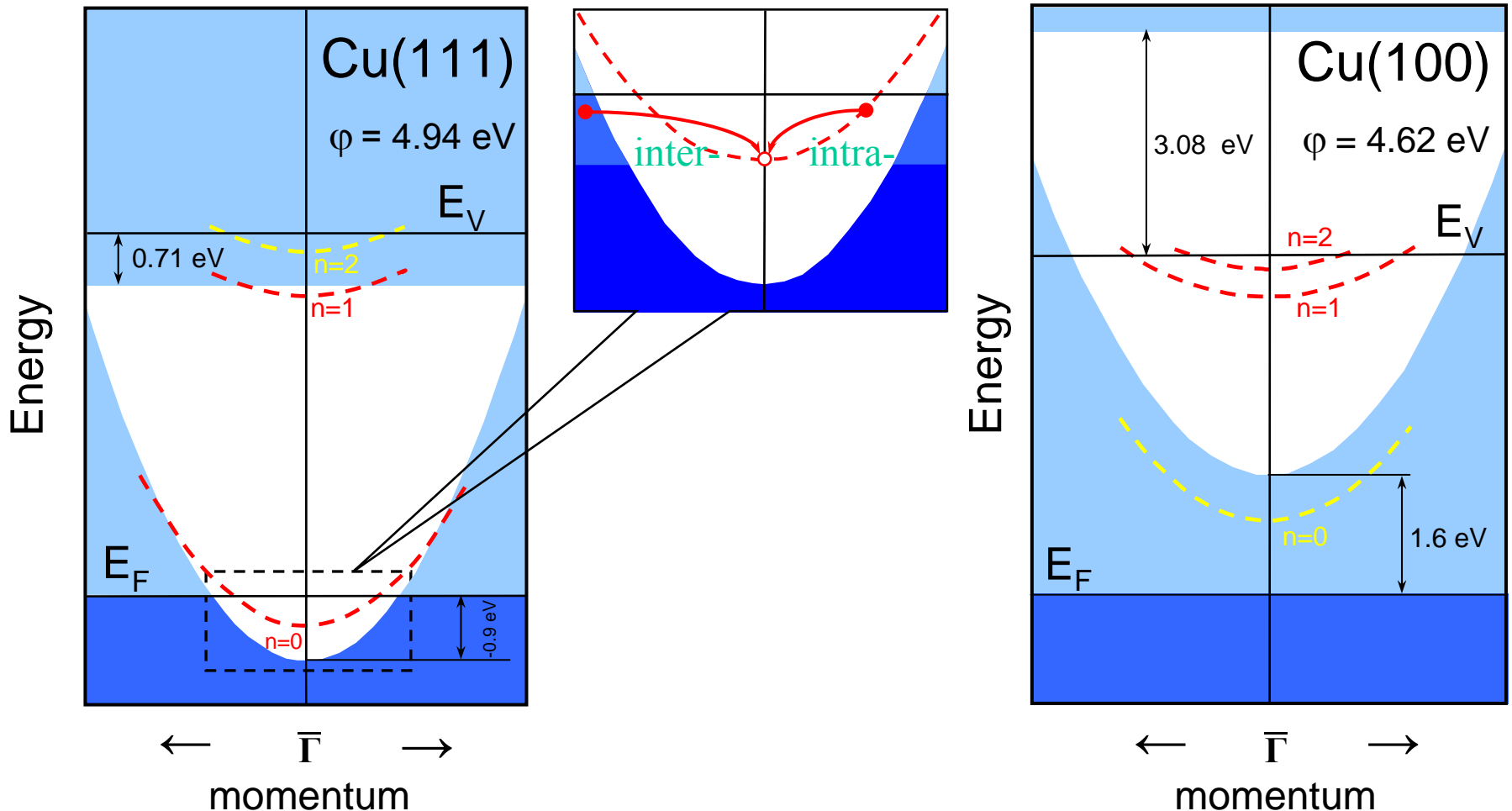
3) Screening: Response Function

$$\text{Im}W(\mathbf{r}, \mathbf{r}'; \omega) = \text{Im}\epsilon^{-1}(\mathbf{r}, \mathbf{r}'; \omega) \cdot V(\mathbf{r} - \mathbf{r}')$$

$\text{Im}\epsilon^{-1}(\mathbf{r}, \mathbf{r}'; \omega)$ is the well known loss function

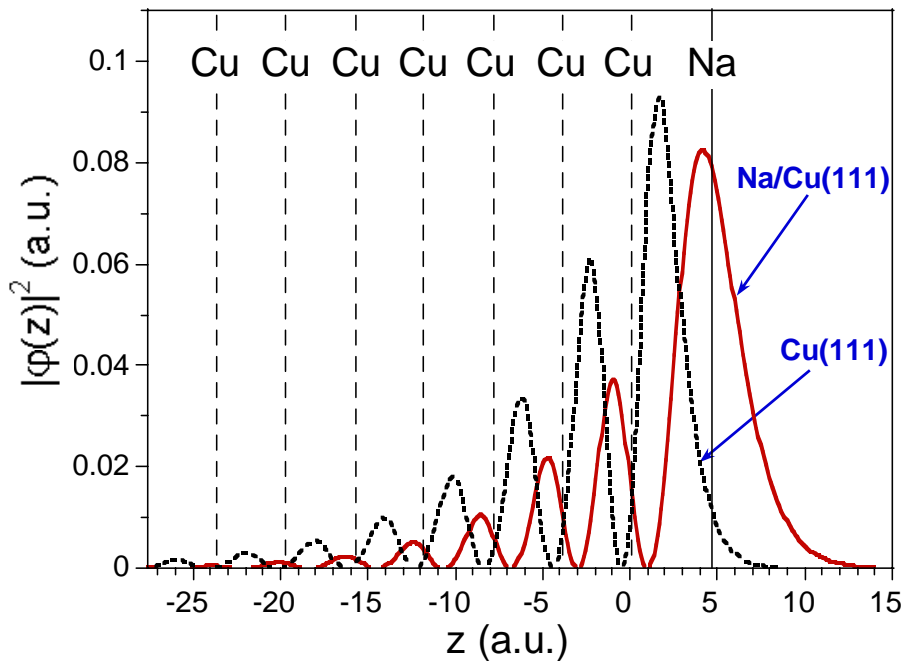
1) Overlap effect: intra- and inter-band transitions

Cu(111) and Cu(100) Surface Band Structures

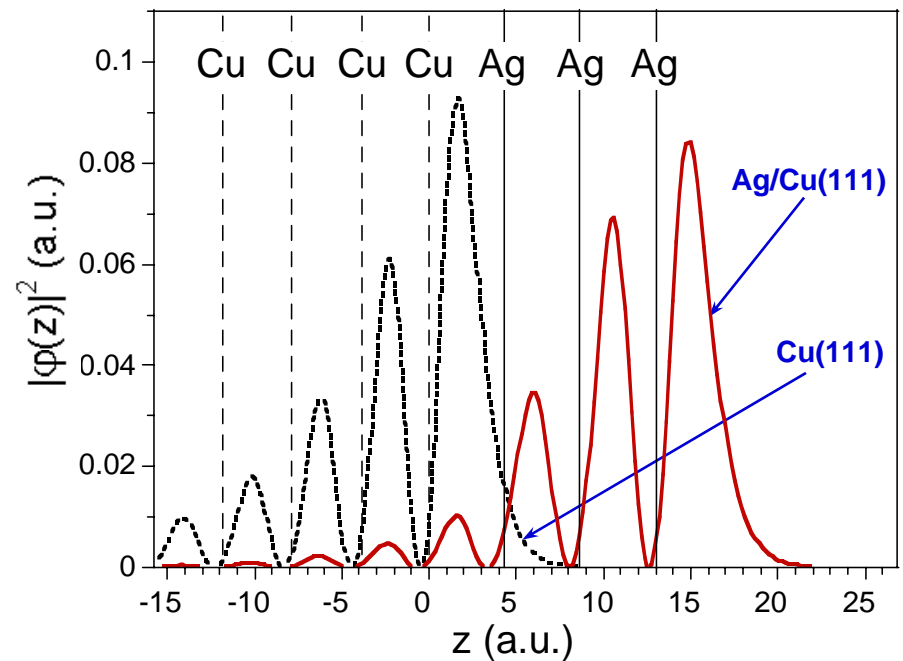


Quantum Well State Charge Density

1ML Na/Cu(111)



3ML Ag/Cu(111)

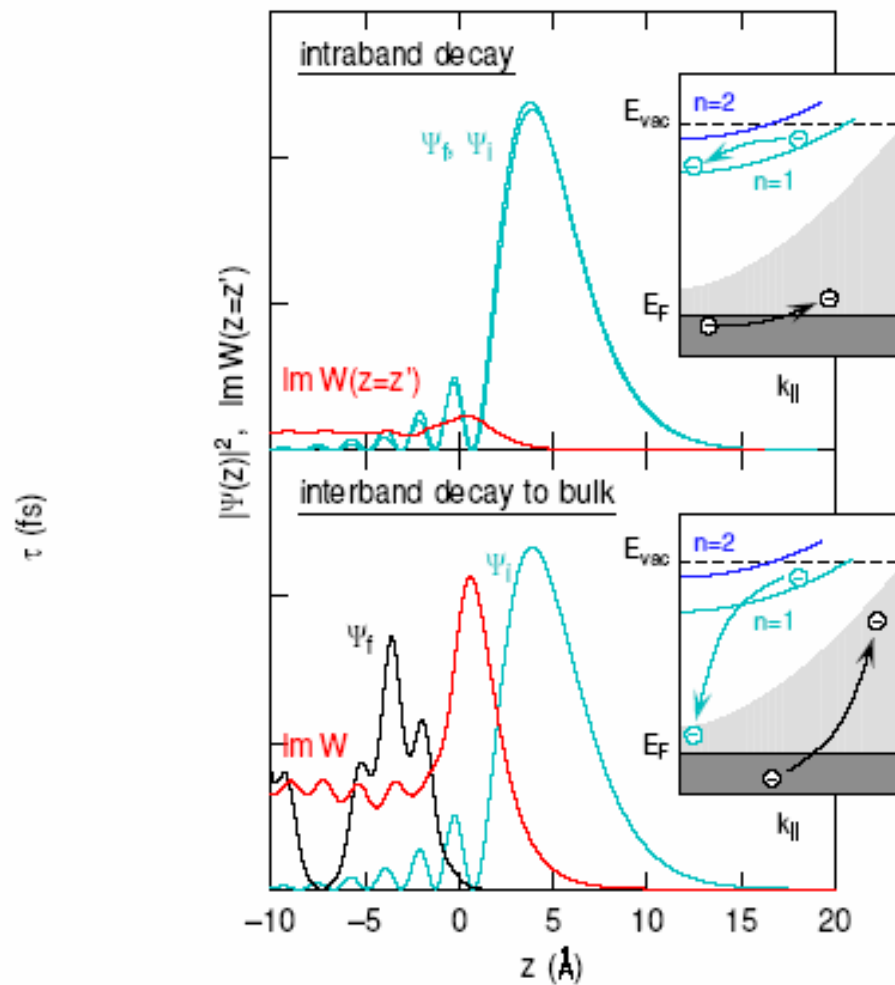
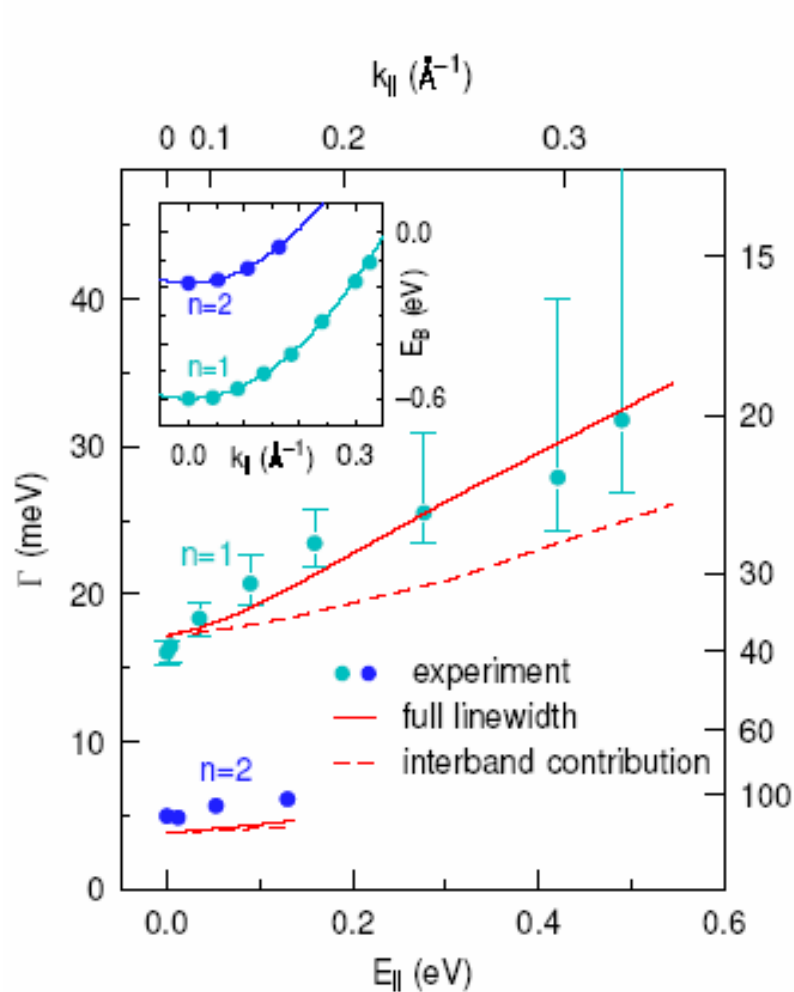


Calculated and measured **inverse lifetime** of the **s-p_z** surface state at the $\bar{\Gamma}$ point on **Cu(111)**. Surface state (**2D**) contribution is indicated in parenthesis. Dominant **2D** effect is also obtained for Ag(111), Au(111), Be(0001), Be(1010). For Mg(0001), Al(111) and Al(100) the **2D** effect is not dominant.

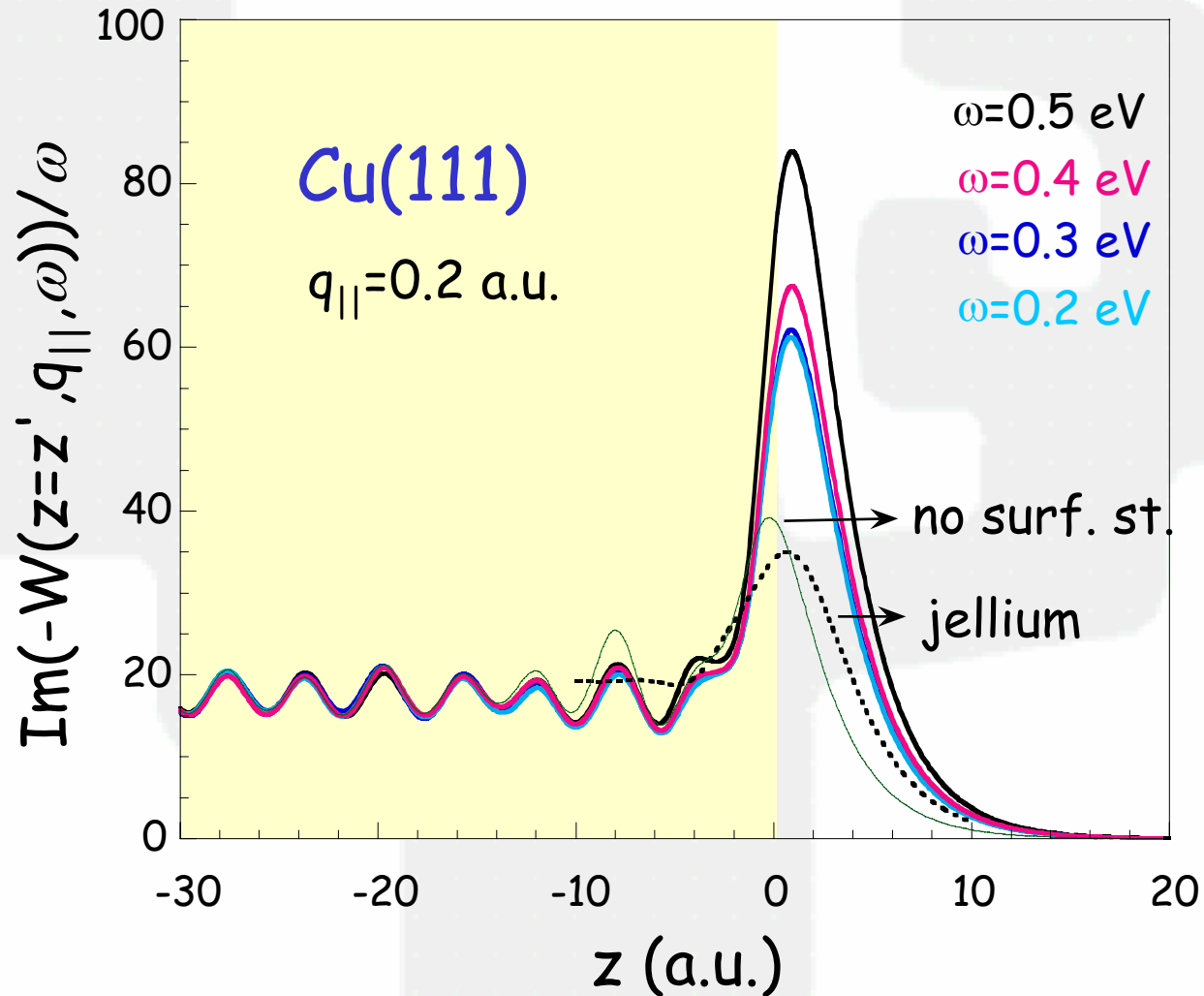
| Temperature | Experimental surface state energy (eV) | Theory Quinn (meV) | Theory Model potential (meV) | Experiment (meV) |
|--------------|--|--|--|---|
| 0 K | -0.44^a | 5 no d-screened | 25(19) no d-screened | Electron contribution 22^b; 16ⁱ |
| 5 K | -0.445ⁱ | 5.1ⁱ d-screened 2.2ⁱ | 25(19)ⁱ d-screened 13.7(11.1)ⁱ | 15^j; 21±5^c Electron+phonon contribution 24ⁱ; 30^b |
| Troom | -0.39^{a,d} | 4 | 23(18) | electron+phonon+defect contributions 55 ± 5^{b,e} ; 65 ± 5^{f,g} 62 ± 4^h |

^aSurf.Sci. **336**, 113 (1995); ^bPhys.Rev. **B51**, 13891 (1995); ^cPhys.Rev. **B56**, 3632 (1997); ^dPhys.Rev. **B36**, 5809 (1987); ^ePhys.Rev.Lett. **50**, 526 (1983); ^fPhys.Rev. **B54**, 14807 (1996); ^gSurf.Sci. **374**, 44 (1997); ^hJ.Electron.Spectrosc.Relat.Phenom.**88-91**, 577 (1988); ⁱScience, **288**, 1399 (2000); ^jPhys.Rev. B **63**, 1154815 (2001)

Momentum-dependent lifetimes of Cu(100)-image-potential states

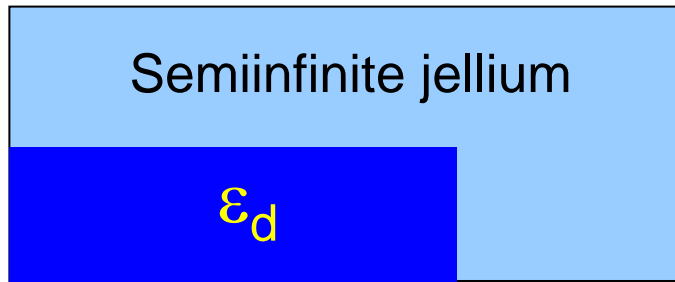


3) Screening: 3D with a mixture of 2D



3) Screening effect: one more aspect

s-d polarization model



A.Liebsch, PRL **71** (1993) 145
(jellium model)



Model potential
+
 ϵ_d d-component of dielectric function
 z_d boundary of d electron medium

Ag: $z_d = -1.5$ a.u. Reproduces
the experimental surface
plasmon dispersion

Inverse lifetime Γ of $n=1$ image state on Ag(100)

Without d-electron effect

$$\Gamma = 18.3 \text{ meV}$$

With d-electron effect

$$\Gamma = 12.0 \text{ meV}$$

Experiment

$$\Gamma = 12 \text{ meV}$$

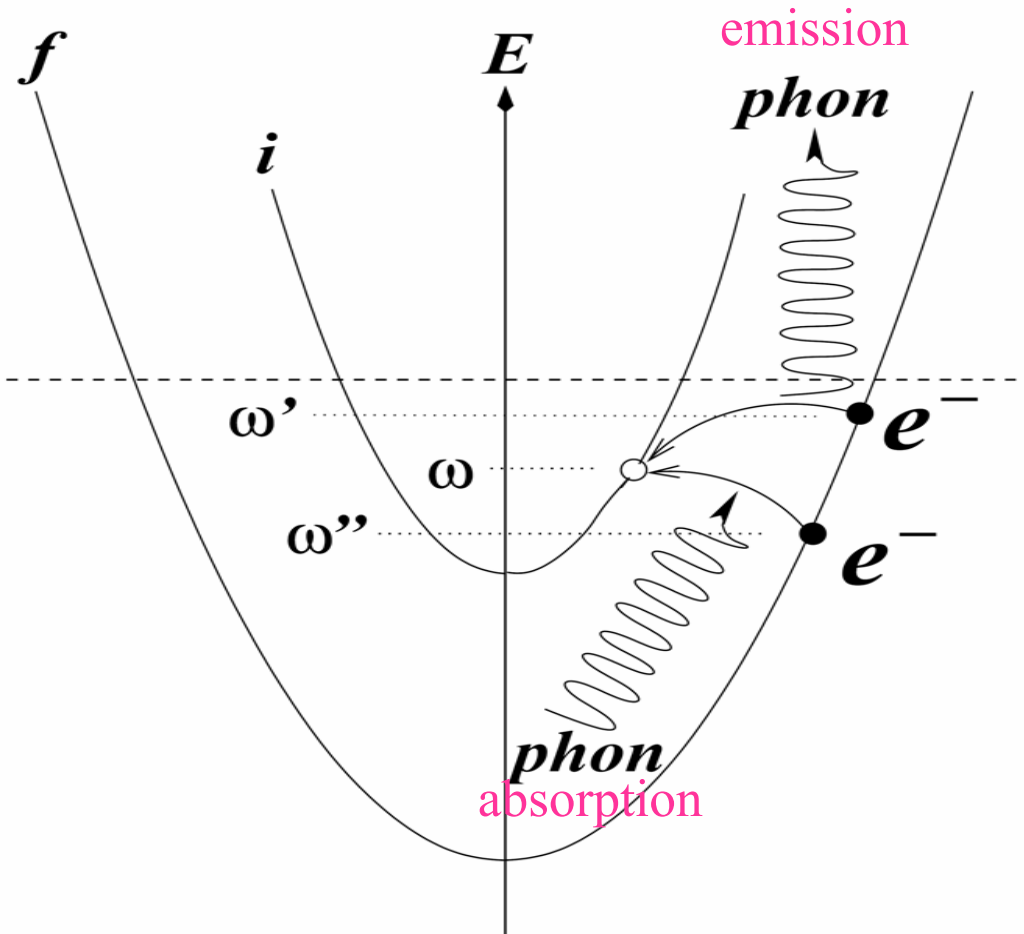
3. Decay mechanisms

PHYSICS OF LIFETIME

(electron-phonon contribution)

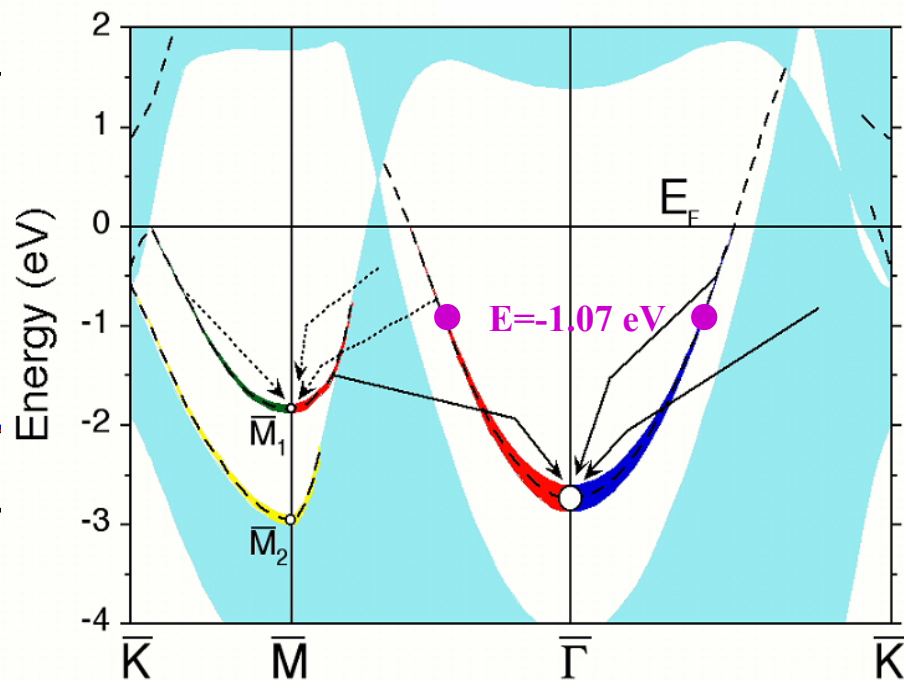
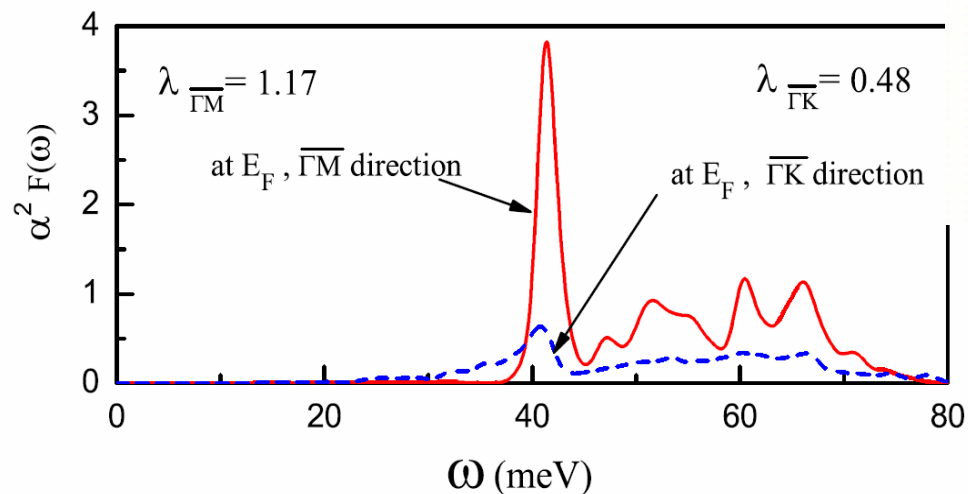
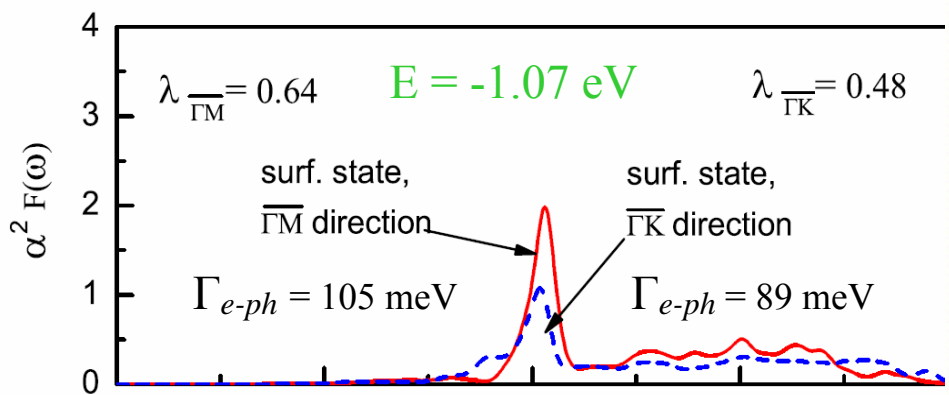
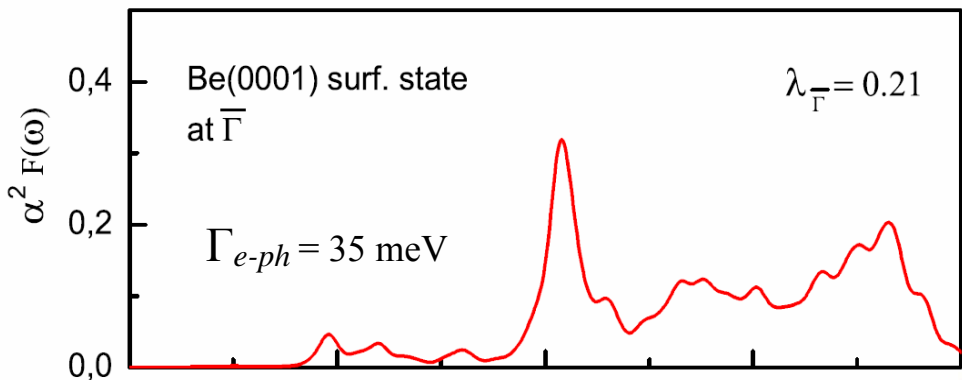
Eliashberg function

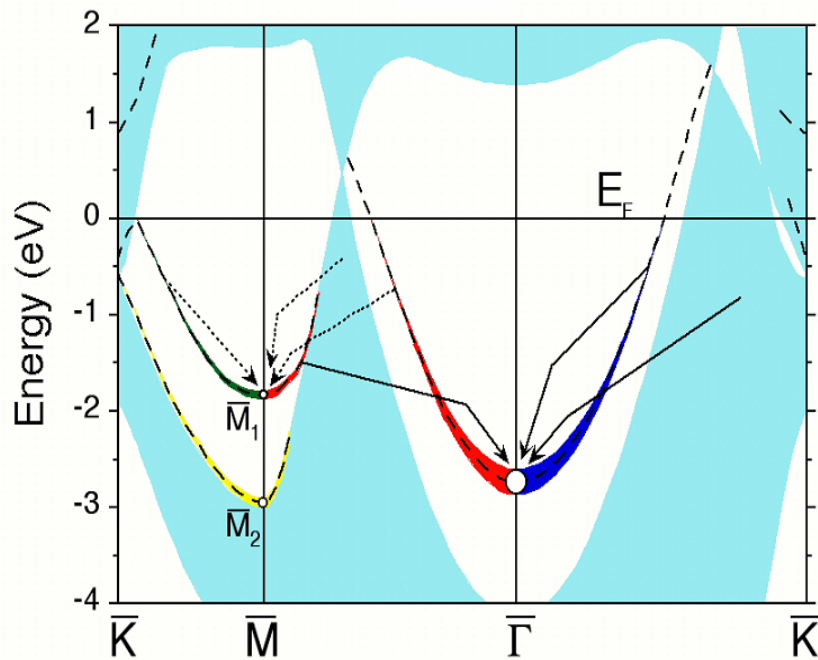
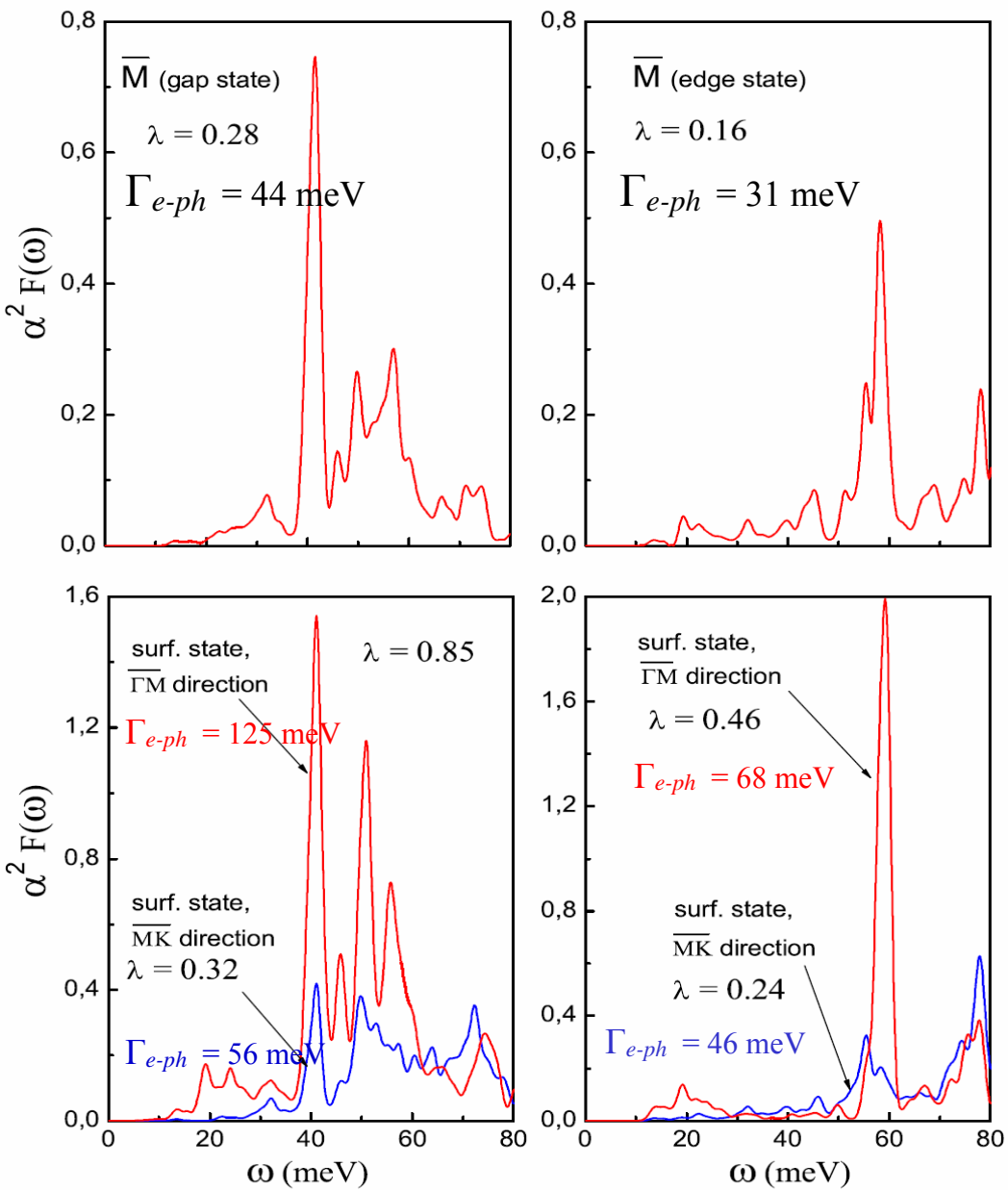
$$\alpha^2 F_{\vec{k}_i}(\omega) \equiv \sum_{\vec{q}, \nu} |g_{\vec{q}, \nu}^{i, f}|^2 \cdot \delta(\varepsilon_{\vec{k}_i}^{el} - \varepsilon_{\vec{k}_f}^{el}) \cdot \delta(\omega - \omega_q^\nu)$$



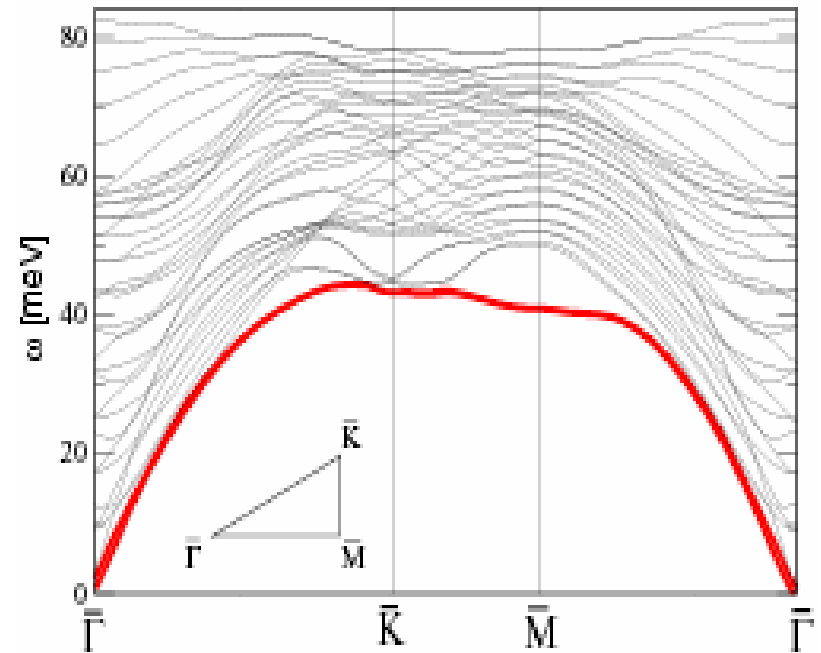
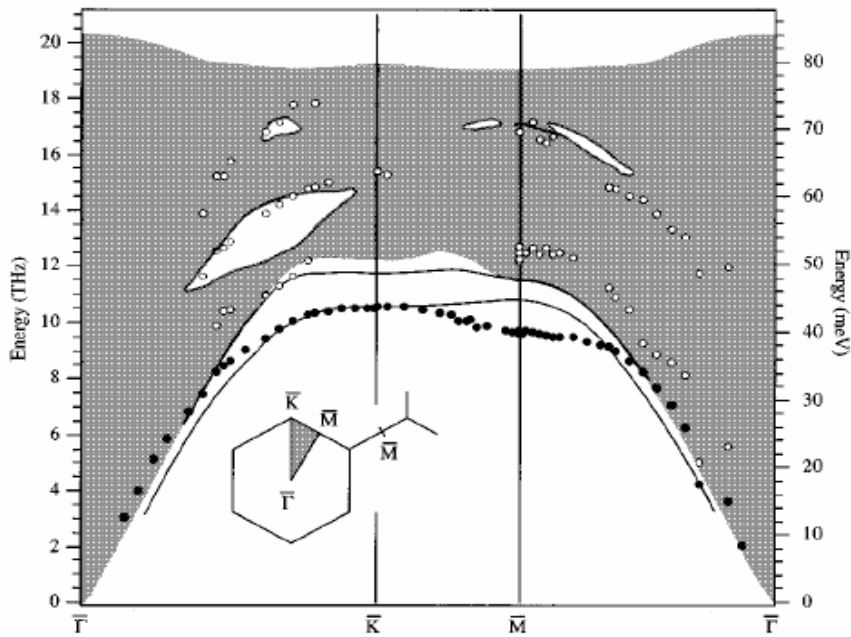
Quasi-elastic approximation

$$\delta(\varepsilon_{\vec{k}_i}^{el} - \varepsilon_{\vec{k}_f}^{el} \pm \omega_q^\nu) \approx \delta(\varepsilon_{\vec{k}_i}^{el} - \varepsilon_{\vec{k}_f}^{el})$$





Measured (left) and calculated (right) surface phonon structure of Be(0001)



J. Hannon, E. J. Mele, and E. W. Plummer,
Phys. Rev **B53**, 2090 (1996)

Our calculation

Summary for the surface states linewidth

Energies (in eV) and linewidths (in meV) for different surface states at low temperatures

| Surface state | | Energy | Γ_{ee} | Γ_{ep} | Γ_{calc} | Γ_{exp} | Calculated | Experimental |
|---------------------|----------------|--------|---------------|---------------|-----------------|----------------|------------|--------------|
| Cu(1 1 1) | $\bar{\Gamma}$ | -0.445 | 14 | 8 | 22 | 24 | [52] | [52] |
| | | -0.435 | | | | 23 ± 1 | | [100] |
| Cu(1 1 0) | \bar{Y} | -0.510 | 8 | | | ≤ 32 | [295] | [127] |
| Ag(1 1 1) | $\bar{\Gamma}$ | -0.067 | 2 | 4 | 6 | 6, 5 | [52] | [52,125] |
| | | -0.063 | | | | 6 ± 0.5 | | [100] |
| Au(1 1 1) | $\bar{\Gamma}$ | -0.505 | 14 | 4 | 18 | 18 | [52] | [52] |
| | | -0.484 | | | | 21 ± 1 | | [100] |
| Be(0 0 0 1) | $\bar{\Gamma}$ | -2.73 | 265 | 80 | 345 | 350 | [143] | [143] |
| Be(0 0 0 1) | \bar{M}_1 | -1.8 | 72 | 80 | 152 | (380) | [143] | [145] |
| Be(1 0 $\bar{1}$ 0) | \bar{A} | -0.42 | 53 | 80 | 133 | 130 | [146] | [146] |
| | | -0.39 | | | | 185 | | [147] |
| Mg(0 0 0 1) | $\bar{\Gamma}$ | -1.6 | 83 | 25 | 108 | (~500) | [53] | [150] |
| | | -1.7 | | | | (~200) | | [144] |
| Al(1 0 0) | $\bar{\Gamma}$ | -2.75 | 131 | 18 | 149 | (500) | [96] | [148] |
| | | | 67 | | | (450) | [295] | [149] |
| Al(1 1 1) | $\bar{\Gamma}$ | -4.56 | 336 | 36 | 372 | (~1500) | [53] | [149] |
| Pd(1 1 1) | $\bar{\Gamma}$ | +1.35 | 37 | | | (54) | [225] | [225] |

The calculated values (Γ_{calc}) are decomposed in electron–electron (Γ_{ee}) and electron–phonon (Γ_{ep}) contributions. Γ_{ep} values for Cu, Ag, Au(1 1 1) and Al(1 0 0) surfaces are from microscopic calculations [95,96], other values from 3D Debye model evaluations for $T = 0$ K. Values for Γ_{exp} in parentheses were measured at room temperature.

Summary for electron-electron contribution to the image-potential states linewidth

Lifetimes τ_n in fs for the n th image-potential state on clean metal surfaces measured by time-resolved two-photon photoemission and calculated using the GW approximation

| | | τ_1 | τ_2 | τ_3 | τ_4 | τ_5 | Refs. |
|-------------|--------------|-------------|--------------|--------------|--------------|--------------|-----------|
| C(0 0 0 1) | Experimental | 40 ± 6 | | | | | [303] |
| Ni(1 1 1) | Experimental | 7 ± 3 | | | | | [304] |
| Cu(0 0 1) | Experimental | 40 ± 6 | 120 ± 15 | 300 ± 20 | 630 | 1200 | [36,218] |
| | Experimental | 41.3 | 150 | 406 | | | [222] |
| | Theoretical | 38 | 168 | 480 | | | [69] |
| Cu(1 1 9) | Experimental | 15 ± 5 | 39 ± 5 | 105 ± 15 | 200 ± 20 | 350 ± 40 | [248] |
| Cu(1 1 7) | Experimental | 15 ± 5 | 39 ± 5 | 95 ± 15 | 190 ± 20 | 350 ± 40 | [248] |
| Cu(1 1 1) | Experimental | 18 ± 5 | 14 ± 3 | 40 ± 6 | | | [221,244] |
| | Theoretical | 29 | | | | | [69] |
| Cu(7 7 5) | Experimental | 18 ± 2 | | | | | [305] |
| Ag(0 0 1) | Experimental | 55 ± 5 | 160 ± 10 | 360 ± 15 | | | [218] |
| | Theoretical | 55 | 219 | 658 | | | [75] |
| Ag(1 1 1) | Experimental | 32 ± 10 | ≤ 20 | | | | [260] |
| | Theoretical | 18 | | | | | [75] |
| Pd(1 1 1) | Experimental | 25 ± 4 | | | | | [225] |
| | Theoretical | 22 | 89 | | | | [225] |
| Pt(1 1 1) | Experimental | 26 ± 7 | 62 ± 7 | | | | [68] |
| | Theoretical | 29 | 73 | | | | [68] |
| Ru(0 0 0 1) | Experimental | 11 | | | | | [267,306] |
| | Theoretical | 14 | | | | | [56] |
| Li(1 1 0) | Theoretical | 18 | 44 | | | | [307] |

Conclusions

1. General conclusion:

now we understand quite many aspects of the physics of electron and hole dynamics.

2. Future:

a) *Ab initio* calculations

b) GW, GW+T-matrix evaluations

c) Electron (hole) dynamics in ferromagnetic materials. New mechanism arises: spin-flip processes (PRL **93**, 096401 (2004))

d) Materials with strong spin-orbit splitting (PRL **93**, 046403 (2004); PRL **93**, 196802 (2004))

In collaboration with:

R. Berndt

Kiel, Germany

T. Balasubramanian

Lund, Sweden

A.G. Borisov, J.P. Gauyacq

Orsay, France

S. Crampin

Bath, England

W. Eberhardt, H. Dürr

Berlin, Germany

P.M. Echenique, J.M. Pitarke,

San Sebastian, Spain

V.M. Silkin, V.P. Zhukov

Th. Fauster,

Erlangen, Germany

B. Hellsing

Göteborg, Sweden

W. Berthold, U. Höfer,

Marburg, Germany

S. Hufner, F. Reinert

Saarbrücken, Germany

K. Kern, A. Schneider,

Stuttgart, Germany

L. Vitali

Yu.M. Koroteev, I.Yu. Sklyadneva

Tomsk, Russia

A. Liebsch, G. Bihlmayer,

Jülich, Germany

S. Blügel